Cell Calcium 82 (2019) 102055

Contents lists available at ScienceDirect

Cell Calcium

journal homepage: www.elsevier.com/locate/ceca

Cytosolic and mitochondrial Ca^{2+} concentrations in primary hepatocytes change with ageing and in consequence of an mtDNA mutation

Jan Niemann, Cindy Zehm, Rica Waterstradt, Markus Tiedge, Simone Baltrusch*

Institute of Medical Biochemistry and Molecular Biology, University Medicine, University of Rostock, Rostock, Germany

ARTICLE INFO

Keywords:
Ca^{2+}
Mitochondria
Hepatocytes
mtDNA mutation
Ageing
MCU

ABSTRACT

Mitochondrial Ca^{2+} flux is crucial for the regulation of cell metabolism. Ca^{2+} entry to the mitochondrial matrix is mediated by VDAC1 and MCU with its regulatory molecules. We investigated hepatocytes isolated from conplastic C57BL/6NTac-mt^{NODLtJ} mice (mtNOD) that differ from C57BL/6NTac mice (controls) by a point mutation in mitochondrial-encoded subunit 3 of cytochrome c oxidase, resulting in functional and morphological mitochondrial adaptations. Mice of both strains up to 12 months old were compared using mitochondrial GEM-GECO1 and cytosolic CAR-GECO1 expression to gain knowledge of age-dependent alterations of Ca^{2+} concentrations. In controls we observed a significant increase in glucose-induced cytosolic Ca^{2+} concentration with ageing, but only a minor elevation in mitochondrial Ca^{2+} concentration. Conversely, glucose-induced mitochondrial Ca^{2+} concentration significantly declined with ageing in mtNOD mice, paralleled by a slight decrease in cytosolic Ca^{2+} concentration. This was consistent with a significant reduction of the MICU1 to MCU expression ratio and a decline in MCUR1. Our results can best be explained in terms of the adaptation of Ca^{2+} concentrations to the mitochondrial network structure. In the fragmented mitochondrial network of ageing controls there is a need for high cytosolic Ca^{2+} influx, because only some of the isolated mitochondria are in direct contact with the endoplasmic reticulum. This is not important in the hyper-fused elongated mitochondrial network found in ageing mtNOD mice which facilitates rapid Ca^{2+} distribution over a large mitochondrial area.

1. Introduction

Intracellular free calcium ions (Ca^{2+}) act as a second messenger and, among other functions, they regulate muscle contractions, signal processing in the brain, cell differentiation and cell death [1]. The cytosolic Ca^{2+} concentration is about 100 nmol/l – 20,000-fold lower than in the extracellular space [2]. During stimulation Ca^{2+} influx from the extracellular space or internal calcium reservoirs, such as the endoplasmic reticulum, can increase the cytosolic Ca^{2+} concentration up to 100-fold [3,4].

In addition, cell metabolism is affected by intra- and extramitochondrial Ca^{2+} concentrations in different ways [5]. Intramitochondrial Ca^{2+} stimulates the pyruvate dehydrogenase complex (PDC), isocitrate dehydrogenase (ICDH) and α-ketoglutarate dehydrogenase (α-KGDH) [6,7], and hence, amplification of the acid cycle and the supply of acetyl-CoA. Extramitochondrial Ca^{2+} activates the aspartate glutamate carrier (AGC) [5], the ATP-Mg/Pi carrier [8] and mitochondrial glycerol phosphate dehydrogenase (mGPD) [9]. However, pathologically elevated cytosolic Ca^{2+} levels stimulate nitric oxide synthases (NOSs) catalysing the production of nitric oxide (NO). NO inhibits cytochrome c oxidase in the respiratory chain, resulting in increased reactive oxygen species (ROS) production at the cytochrome bc1 complex [10]. ROS also oxidise cardiolipin in the inner mitochondrial membrane, thus promoting cytochrome c release. Furthermore, pathological Ca^{2+} levels directly stimulate cytochrome c release because of concurrent activity at the cardiolipin binding site [11]. Finally, high Ca^{2+} levels support formation of the mitochondrial permeability transition pore (mPTP) through which cytochrome c can flow into the cytosol and initiate apoptosis [12,13].

The voltage-dependent anion-selective channel (VDAC1) in the outer mitochondrial membrane and the mitochondrial calcium uniporter (MCU) in the inner mitochondrial membrane are key components for Ca^{2+} shuttling from the cytosol into mitochondria [14,15]. MCU activity is regulated by a heterodimer composed of the proteins mitochondrial calcium uptake 1 and 2 (MICU1 and MICU2), MCU regulator (MCUR1), MCU regulator EMRE (mouse Smdt1). MCUR1 and

Abbreviations: mtNOD, C57BL/6NTac-mt^{NODLtJ} mice; controls, C57BL/6NTac mice; MCU, Mitochondrial calcium uniporter; MICU1, Mitochondrial calcium uptake 1; MCUR1, MCU regulator

* Corresponding author at: Institute of Medical Biochemistry and Molecular Biology, University Medicine, University of Rostock, D-18057 Rostock, Germany.
E-mail address: simone.baltrusch@med.uni-rostock.de (S. Baltrusch).

https://doi.org/10.1016/j.ceca.2019.102055
Received 25 March 2019; Received in revised form 12 June 2019; Accepted 16 July 2019
Available online 26 July 2019

Smdt1 are reported to have a direct positive impact on Ca^{2+} uptake via the MCU [16–20]. However, another study has shown that MCUR1 is a cytochrome c oxidase assembly factor rather than a regulator of the MCU [21]. At low cytosolic Ca^{2+} levels MICU2 shuts down MCU activity, whereas at high Ca^{2+} levels stimulated MICU1 supports MCU activity [22]. The molecular regulation of MCU and its implications in physiology and disease have recently been reviewed in detail [23]. In addition, the mitochondrial solute carrier SLC25A23 stimulates MCU activity. However, SLC25A23 plays a dual role and also induces oxidative stress-mediated cell death [24].

Regulation and adaptation of mitochondrial Ca^{2+} influx is therefore crucial for cellular metabolism and viability. In a recent study we demonstrated causality relationships between a single subunit 3 of cytochrome c oxidase (COX 3) mutation and age-dependent ROS production, mitochondrial dynamics and metabolism at the cellular level of primary hepatocytes [25]. COX 3 is encoded by the mitochondrial DNA and is pivotal for cytochrome c oxidase activity [26]. The conplastic C57BL/6NTac-mt$^{NOD/LtJ}$ (mtNOD) mouse strain used for the experiments carries the mitochondrial DNA from the NOD/LtJ-strain with an nt9821-10A and an nt9348A polymorphism in COX 3 but the same nuclear DNA as the C57BL/6NTac mouse strain that served as control [25,27]. Control and mtNOD mice showed an increase in mitochondrial ROS generation from the age of 3 to 9 months [25]. Different mitohormesis was associated with decreasing ROS production beyond 9 months in controls, but with constantly high levels in mtNOD mice [25]. In controls the mitochondrial membrane potential and ATP production showed a slight decline from the age of 3 to 12 months [25]. mtNOD mice had a significantly lower membrane potential and reduced ATP production compared with controls at the age of 3 months. However, both parameters increased stepwise with age [25]. The aim of the present study was therefore to investigate cytosolic and mitochondrial Ca^{2+} concentrations and expression of the specific Ca^{2+} transporter in hepatocytes of mtNOD and control mice.

2. Materials and methods

2.1. Experimental animals

The conplastic C57BL/6NTac-mt^{NODLtJ} (mtNOD) mouse strain was generated by crossing females from the mitochondrial donor strain (NOD/LtJ) to males with the preferred genomic background (C57BL/6NTac), as described [25,27]. The background strain served as controls in this study. Mice were housed at the central animal care facility of the Rostock University Medicine, receiving conventional rodent chow (SSNIFF) and water *ad libitum*. The colonies were regularly monitored for murine pathogens, in line with the recommendations of the Federation for Laboratory Animal Science Associations. This study was carried out in accordance with the German Animal Welfare Act 2006 (last amended 2014) and has been approved by the State Department of Agriculture, Food Safety and Fisheries, Mecklenburg-Vorpommern (LALLF M–V). Only male mice were used for hepatocyte isolation.

2.2. Isolation of primary hepatocytes

Hepatocytes were isolated, as described [28], from 3-, 6-, 9- and 12-month-old male control and mtNOD mice and used directly for RNA isolation or seeded on glass-bottom dishes (MatTak Corporation, Ashland, MA, USA) and cultured in Williams Medium E (Merck, Darmstadt, Germany) supplemented with fetal calf serum (10%), penicillin-streptomycin (1%), glutamine (2.5%), insulin (0.5%) and dexamethasone (0.01%) (Life technologies, Carlsbad, CA, USA) for one day prior to transfection.

2.3. Measurements of subcellular Ca^{2+} concentration in primary hepatocytes

Hepatocytes were transfected with 2 µg DNA (equal ratio of plasmids) and 6.4 µl PromoFectine Hepatocyte (PromoKine, Heidelberg, Germany) according to the manufacturer's instructions. For subcellular resolution of changes in the Ca^{2+} concentration, cytoplasmic localised CAR-GECO1, mitochondrial localised CAR-GECO1 [29] (Addgene, Teddington, UK) and mitochondrial localised GEM-GECO1 protein [30] (Addgene) were expressed under control of a CMV promoter. The Ca^{2+}-dependent fluorescence intensity change of these sensors is based on Ca^{2+} binding to calmodulin. The intensity of CAR-GECO1 proteins was 10-fold and that of GEM-GECO1 2-fold higher in the Ca^{2+}-bound state in our experiments. For Ca^{2+}-independent visualisation of the mitochondrial network the previously generated mitochondrial localised TagBFP vector was used [31,32]. One day after transfection the medium was exchanged and the hepatocytes were cultured for a further day. Finally, cells were starved for one hour in Krebs-Ringer solution.

Ca^{2+} measurements were carried out using an xcellence/Olympus IX81 microscope system (Olympus, Hamburg, Germany) equipped with a Cellcubator (Olympus) to maintain 60% humidity, 37 °C, and 5% CO_2, an UPLSAPO 60 × 1.35 numerical aperture oil-immersion objective (Olympus) and OrcaR^2 CCD camera (Hamamatsu Corporation, Bridgewater/NJ, USA) and 387/11 and 556/20 bright line HC excitation filters, 403/497/574 HC triple beam splitter plus 433/517/613 HC triple band emission filter (F66-512) and HC BS 409 beam splitter plus 510/84 bright line HC excitation filter (F76-520, AHF Analysentechnik, Tübingen, Germany). Two-channel image acquisitions were performed by continual alternation at a speed of 650 ms (mitochondrial CAR-GECO1 and TagBFP) and 950 ms (cytoplasmic CAR-GECO1 and mitochondrial GEM-GECO1) per channel. Cells were incubated for the first two minutes of the experiments in Krebs-Ringer solution without glucose and thereafter with 25 mmol/l glucose. Time-resolved fluorescence intensity changes were calculated using the xcellence software and normalised to the starting point.

2.4. Gene expression analyses

Hepatocytes were homogenised in QIAshredder Mini Spin Columns (Qiagen, Hilden, Germany) by centrifugation (2 min, 12,000 rpm). Thereafter RNA was isolated and purified with the RNeasy® Mini Kit (Qiagen). cDNA was synthesized using the Maxima™ First Strand cDNA synthesis kit for RT-qPCR (Thermo Scientific, Darmstadt, Germany). RNA solutions containing the probes of the cDNA synthesis kit were placed in a thermocycler (Labcycler, SensoQuest, Göttingen, Germany) programmed at 25 °C for 10 min, followed by 50 °C for 15 min and by 85 °C for 5 min. For real-time PCR, cDNA solutions containing TaqMan Universal Master Mix (Applied Biosystems, Darmstadt, Germany) and one of the following TaqMan® Gene Expression Assays (MCU Mm03951306_g1, MICU1 Mm00522778_m1, MICU2 Mm00551312_m1, MCUR1 Mm01351578_m1, Smdt1 Mm01306306_m1, SLC25A23 Mm01232022_m1, VDAC1 Mm01288627_g1, Applied Biosystems) of primer and gene probe were amplified and detected using a 7900 H T Fast Real-Time System (Life Technologies, Darmstadt, Germany). The PCR system was programmed at 50 °C for 2 min, followed by 95 °C for 10 min and by 40 repeats of the steps 95 °C for 15 s and 60 °C for 1 min. GAPDH served as a housekeeping gene (Mm99999915_g1, Applied Biosystems). Gene expression values were calculated with the SDS RQ Manager 1.2 software (Life Technologies).

2.5. Protein expression analyses

For western blot analyses 40 µg of cellular proteins were separated by SDS-PAGE and blotted onto Roti®-Fluoro PVDF membrane (Carl Roth, Karlsruhe, Germany). Membranes were probed for two hours at

37 °C with anti-MCU (Abbexa, Cambridge, UK, abx325243, 1:1500), anti-MICU1 (antibodies-online, Aachen, Germany, ABIN1804714, 1:500), anti-VDAC1 (Acris, Herford, Germany, AP00265PU-N, 1:500) and anti-actin (Cell Signaling Technology, Frankfurt, Germany, 4970, 1:1000) antibodies. Immunoreactive bands were visualised using IRDye 680, IRDye 800 CW fluorescence-labelled secondary antibodies and analysed via the Odyssey imaging system. Densitometry measurements of bands were performed using the Odyssey infrared imaging system (LI-COR, Lincoln, NE, USA) and the MICU1/MCU ratio was calculated.

For immunofluorescence staining hepatocytes were fixed with 4% formaldehyde for 15 min and permeabilised with 0.2% Tween 20 for 5 min in phosphate-buffered saline. Cells were stained for two hours with anti-MICU1 (antibodies-online, Achen, Gernamy, ABIN1804714, 1:50) and anti-TOMM20 (Abcam, Cambridge, UK, ab186735, 1:50) antibody. Positive signals were visualised using Alexa488 or Alexa594 (Abcam, Cambridge, UK, 1:250). The samples were counterstained with DAPI by using Roti®-Mount FluorCare DAPI (Carl Roth; Karlsruhe, Germany) for mounting. Images were generated using the FV10i confocal microscope and FV10-ASW software (Olympus).

2.6. Statistical analysis

Statistical analyses were performed using the Prism® 5.00 analysis program (GraphPad, San Diego, CA, USA) and the results are presented as means ± SEM. Unless otherwise stated, differences were examined using ANOVA/Bonferroni's correction, and p values < 0.05 were considered to be statistically significant.

3. Results

3.1. Age-dependent effects on cytosolic and mitochondrial Ca^{2+} concentrations in primary hepatocytes after glucose stimulation

Transient transfections resulted in comparable expression of both CAR-GECO1 and GEM-GECO1 in hepatocytes of mtNOD and control mice. The fluorescence of the Ca^{2+} sensor proteins remained stable during the experiments and was not affected by addition of Krebs-Ringer solution (data not shown). It should be noted that for clarity, the results of co-transfection experiments are shown in separate figures and only every seventh measurement point is presented in the curves (Fig. 1A–D, Fig. 2A–D). After addition of glucose we observed an increase in both cytosolic and mitochondrial Ca^{2+} in hepatocytes starved for 1 h, falling to baseline levels after 3–6 min (Fig. 1A–D, Fig. 2A–D). For calculations of Ca^{2+} concentrations (Figs. 1E, 2 E) we therefore quantified the area under curve over the first 3 min. A significant stepwise increase in cytosolic Ca^{2+} concentration with ageing was noted in control mice (Fig. 2E), whereas an oscillatory pattern with higher values at 3 and 9 months was observed in mtNOD mice. A significant difference was observed at 12 months, with values in controls twice as high as in mtNOD mice (Fig. 1E). Mitochondrial Ca^{2+} concentration in control mice was stable with a tendency to higher values from 6 months onwards (Fig. 2E). In contrast, a decrease with ageing was observed in mtNOD mice, with significantly different values between 3 and 12 months (Fig. 2E). At 3 months mtNOD mice showed significantly higher Ca^{2+} concentration than controls (Fig. 2E).

3.2. Measurement of mitochondrial Ca^{2+} concentration in primary hepatocytes

Further experiments were performed in hepatocytes from 3-month-old mice: after Ca^{2+} binding the CAR-GECO1 protein exhibits a greater intensity increase than the GEM-GECO1 protein, but is susceptible to pH and ion concentration. Higher Ca^{2+} concentration was detected in hepatocytes of mtNOD mice than in controls (Fig. 3), as already observed with the GEM-GECO1 protein (Fig. 2). Additional experiments were conducted using co-transfection with a construct that localises the very stable TagBFP fluorescence protein to the inner mitochondrial membrane [32]. In both strains mitochondrial TagBFP fluorescence did not change following addition of glucose, whereas the rise in intensity of the CAR-GECO1 protein was clearly detectable (Fig. 4). Notably, the greatest increase occurred in mitochondria in the centre of the cell close to the nucleus (Fig. 4). This finding was confirmed when mitochondrial Ca^{2+} concentrations were calculated on the basis of organelle-specific TagBFP fluorescence (Fig. 5).

3.3. Expression of Ca^{2+} channels changes with age in primary hepatocytes

Gene expression of the MCU in liver was comparable in 3-month-old animals of both strains, but was significantly higher in 9- and 12-month-old mtNOD mice than in controls. With ageing, no changes in MCU expression were detectable in controls, whereas significantly increased expression was noted in mtNOD mice, with the highest values observed at 9 months (Fig. 6A). At 3, 6 and 9 months, gene expression levels of VDAC1 were comparable in both strains (Fig. 6B). By contrast with the significant decrease in gene expression of VDAC1 in controls at 12 months, levels remained unchanged in mtNOD mice. Gene expression levels of five MCU regulatory subunits – MICU1, MICU2, MCUR1, Smdt1 and SLC25A23 – revealed opposite trends with ageing in control and mtNOD mice (Fig. 6C–G). MICU1 and SLC25A23 expression decreased in controls but increased in mtNOD mice. Disregarding slight differences in the pattern of MICU1 and SLC25A23 expression, significant differences between mtNOD and control mice were observed at 3 and 12 months (Fig. 6C, D). MICU2 and Smdt1 expression were virtually stable with ageing in both strains, but showed a tendency to lower values in 12-month-old control mice (Fig. 6E, F). The age-dependent expression pattern of MCUR1 differed from those observed for the other regulators in both strains (Fig. 6G). Increased expression was noted up to 9 months in control mice, followed by a significant decrease at 12 months. MCUR1 expression was significantly higher in 3-month-old mtNOD mice than in controls. However, a stepwise decrease with ageing was noted with significantly lower expression in 12- than in 3-month-old mtNOD mice and compared with controls at 9 months (Fig. 6G). Notably, the same pattern was observed for the MICU1/MCU ratio (Fig. 6H). Immunofluorescence staining and subsequent confocal microscopy showed MICU1 protein expression and colocalisation with the more fragmented mitochondrial network in hepatocytes of control animals (Fig. 7A) and the elongated mitochondrial structures in mtNOD mice at the age of 12 months (Fig. 7B). Western blot analyses (Fig. 7C) confirmed a lower MICU1/MCU ratio in mtNOD mice than in controls at the protein level.

4. Discussion

Intense interest is currently focused on how ageing is affected by mutations in the mitochondrial genome encoding subunits of the respiratory chain complexes. The conplastic C57BL/6NTac-mt^{NODLtJ} mice differed from C57BL/6NTac mice by a point mutation in mitochondrial-encoded COX 3 [25,27]. By investigating hepatocytes from both strains we have previously demonstrated that only the conplastic strain developed elongated mitochondrial networks with artificial loop structures, depressed autophagy, high mitochondrial respiration and ROS accumulation as well as an up-regulated antioxidative response in middle and late age [25]. While cytosolic and mitochondrial Ca^{2+} changes appear to play an important regulatory role in this context that will shed light on the observed pathological findings, this aspect has not yet been adequately explored.

A study comparing isolated mitochondrial fractions revealed tissue-specific Ca^{2+} tuning in the heart and liver of mice that is important for specific organ function [33]. However, use of isolated mitochondria does not permit investigation of either cellular metabolic adaptations or the impact on Ca^{2+} flux of mitochondrial network architecture and contact sites with the endoplasmic reticulum. Acute alcohol treatment

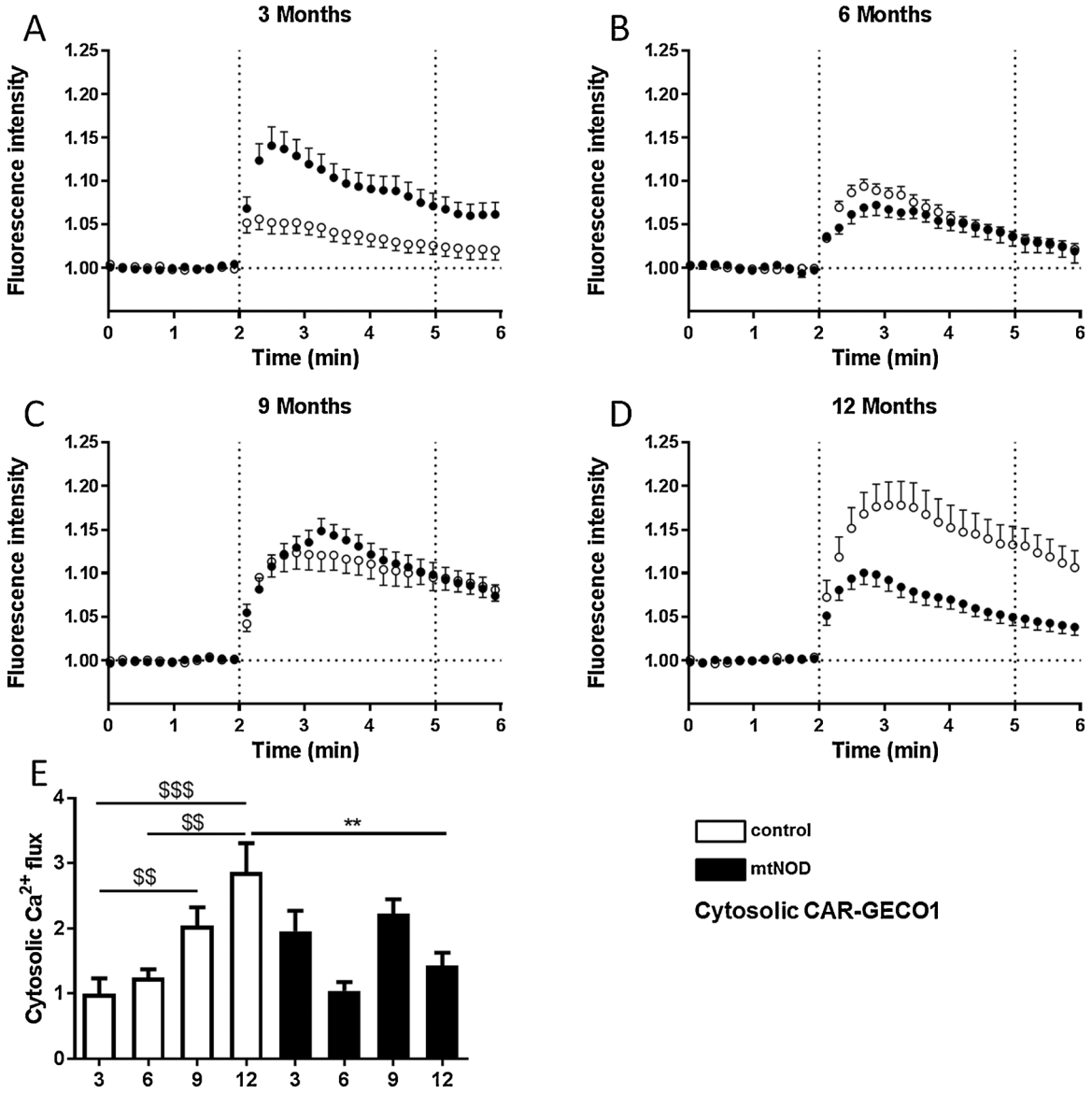

Fig. 1. Cytosolic Ca^{2+} changes in primary hepatocytes after glucose supply. Cytosolic Ca^{2+} was measured using the CAR-GECO1 protein. After two minutes glucose was added to a final concentration of 25 mmol/l. Hepatocytes from 3- (A), 6- (B), 9- (C), and 12-month-old (D) control mice (white circles) and mtNOD mice (black circles) were investigated. Fluorescence intensities measured at the starting point were not significantly different between age groups and both mouse strains. Mean normalised value curves ± SEM are shown for 9–18 hepatocytes from 3 mice per age category and group. (E): In a final step the area under curve was determined from minute 2 to 5 relative to baseline (minute 0 to 2); these are shown for control mice (white bars) and mtNOD mice (black bars) as mean values ± SEM normalised to 3-month-old control mice (**, $$ $p < 0.01$; $$$ $p < 0.001$; 1-way ANOVA/Bonferroni's test). Results were determined together with mitochondrial Ca^{2+} measurements shown in Fig. 2.

has been shown to evoke changes in mitochondrial Ca^{2+} handling and an increase in cytosolic Ca^{2+} in rat hepatocytes [34]. We studied the response to a carbohydrate supply after starvation and found both glucose-induced cytosolic and mitochondrial Ca^{2+} influx in hepatocytes of both mouse strains. Assuming conditions with adequate oxidative capacity in primary mouse hepatocytes, this could have been expected as an adaptation towards an enhanced metabolism rate [7]. Thus, we confirmed that an increased cytosolic Ca^{2+} concentration stimulates cell respiration on various levels [35].

Because of the permanent shift in pH and ion concentration in the mitochondrion, the use of organelle-targeted fluorescence-based Ca^{2+} sensors deserves serious evaluation so that robust results can be obtained. GEM-GECO1 appears to fulfil this requirement because it has been recently shown that the protein is even suitable for Ca^{2+} measurements in endosomes, i.e. in organelles with a highly acidic nature [36]. Its use alongside CAR-GECO1 as a cytosolic Ca^{2+} sensor revealed different age-dependent changes in glucose-induced cytosolic and mitochondrial Ca^{2+} concentrations in controls. By contrast with a slight increase in mitochondrial Ca^{2+} concentration in hepatocytes, cytosolic Ca^{2+} concentration was significantly raised. With ageing, therefore, cytosolic (but not mitochondrial) processes in hepatocytes require further signal amplification by Ca^{2+} after glucose uptake. The uncoupled cytosolic and mitochondrial Ca^{2+} changes from the age of 9 to 12 months can be explained by the decrease in MICU1, MICU2, Smdt1, MICUR1 and SLC25A23 to MCU expression with ageing (Fig. 6) and the slight decrease in mitochondrial membrane potential [25]. Interestingly, the pattern of MICUR1 expression parallels ROS production [25] with an increase up to 9 months and a decline at 12 months. Moreover, VDAC1 gene expression was lower at 12 months. This should reduce the permeability of both the inner and the outer mitochondrial membrane for Ca^{2+}. Taken together, these findings are in line with our previous results in the C57BL/6NTac control strain where we observed a decline

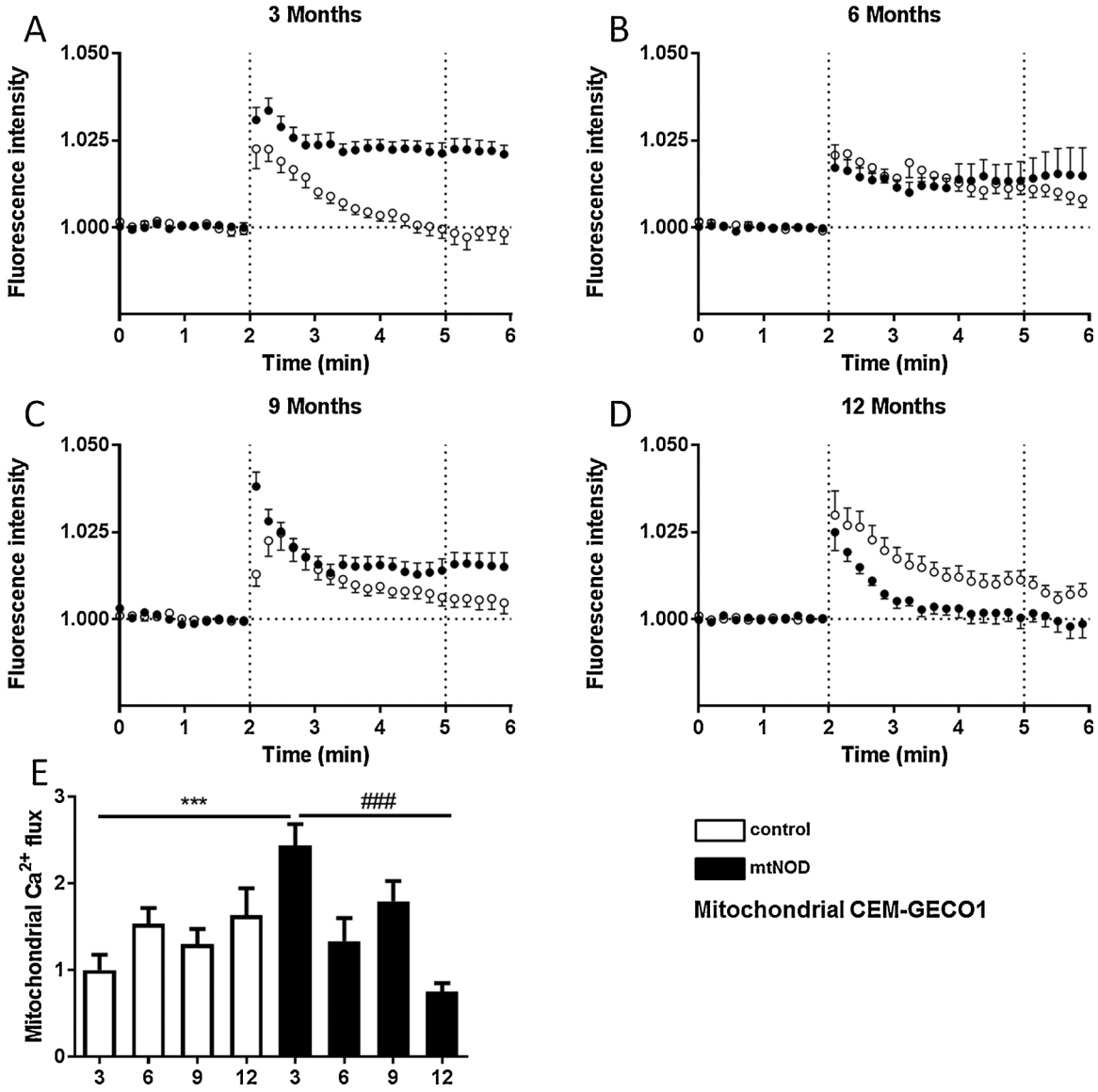

Fig. 2. Mitochondrial Ca^{2+} changes in primary hepatocytes after glucose supply. Mitochondrial Ca^{2+} was measured using the GEM-GECO1 protein. After two minutes glucose was added to a final concentration of 25 mmol/l. Hepatocytes from 3- (A), 6- (B), 9- (C), and 12-month-old (D) control mice (white circles) and mtNOD mice (black circles) were investigated. Fluorescence intensities measured at the starting point were not significantly different between age groups and both mouse strains. Mean normalised value curves ± SEM are shown for 9–18 hepatocytes from 3 mice per age category and group. (E): In a final step the area under curve was determined from minute 2 to 5 relative to baseline (minute 0 to 2); these are shown for control mice (white bars) and mtNOD mice (black bars) as mean values ± SEM normalised to 3-month-old control mice (***, ### $p < 0.001$ 1-way ANOVA/Bonferroni's test). Results were determined together with cytosolic Ca^{2+} measurements shown in Fig. 1.

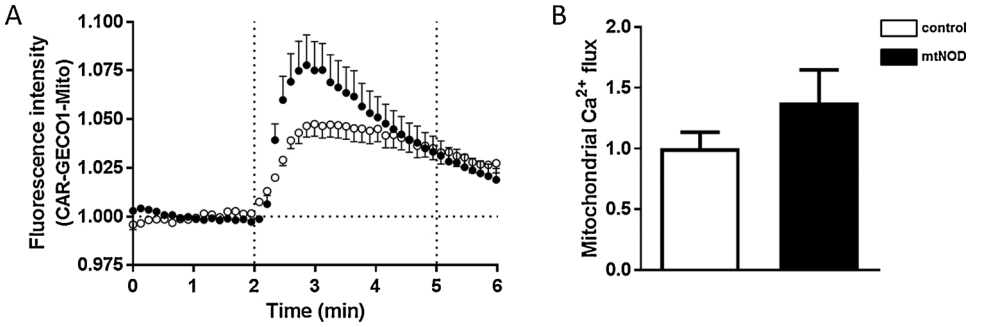

Fig. 3. Mitochondrial Ca^{2+} changes in primary hepatocytes after glucose supply. Mitochondrial Ca^{2+} was measured using the CAR-GECO1 protein. After two minutes glucose was added to a final concentration of 25 mmol/l. Hepatocytes from 3-month-old control mice (white circles) and mtNOD mice (black circles) were investigated (A). Fluorescence intensities measured at the starting point were not significantly different between both mouse strains. Mean normalised value curves ± SEM are shown for 9 hepatocytes from 3 mice per age category and group. (B): In a final step the area under curve was determined from minute 2 to 5 relative to baseline (minute 0 to 2); these are shown for control mice (white bars) and mtNOD mice (black bars) as mean values ± SEM normalised to 3-month-old control mice.

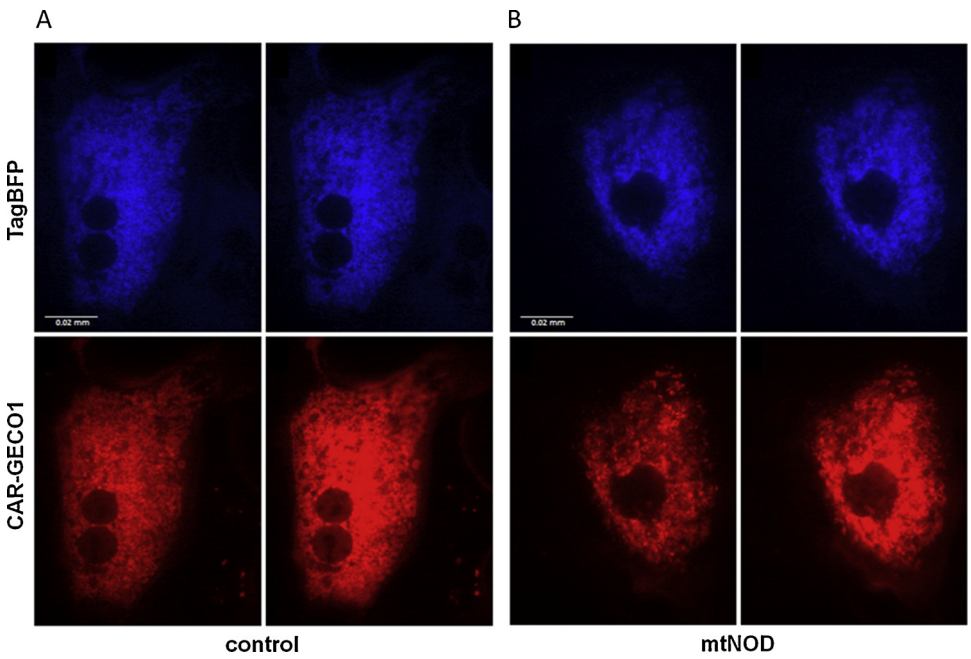

Fig. 4. Representative images of hepatocytes from 3-month-old control mice (A) and mtNOD mice (B). Hepatocytes transiently express the mitochondrial localised TagBFP (blue, upper row) and CAR-GECO1 Ca^{2+} sensor (red, lower row) proteins. The left-hand image in each sequence pair was taken after starvation at the beginning of the measurement; the right-hand image in each pair shows the cell after glucose supply at minute 3 of the experiment. Scale bar: 20 µm.

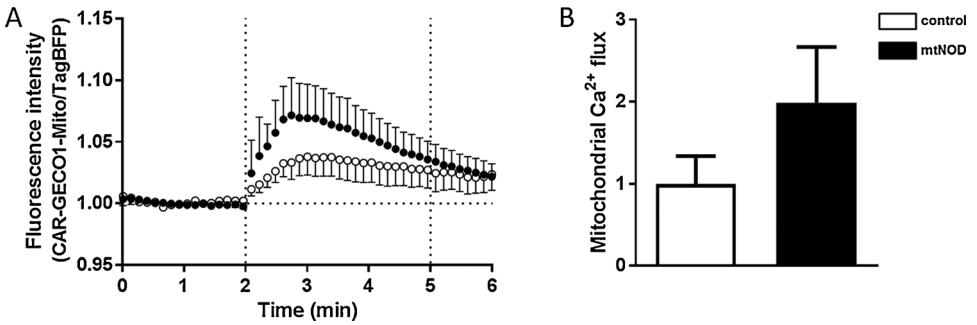

Fig. 5. Changes in mitochondrial Ca^{2+} concentration calculated on the basis of organelle-specific TagBFP fluorescence. The mitochondrial Ca^{2+} changes presented in Fig. 3 were normalised to the co-expressed mitochondrial localised fluorescent TagBFP protein for each measurement point.

in the total mitochondrial metabolism rate but sufficient energy supply [25]. This was accompanied by a more fragmented mitochondrial network [25] (Fig. 7). In the presence of many single mitochondria rather than an interconnected network, it can be assumed that only some will have direct contact with the endoplasmic reticulum and ultimately that Ca^{2+} influx will vary widely among the mitochondrial population [37]. It can further be hypothesised that the higher cytosolic Ca^{2+} concentration with ageing is necessary to maintain an adequate level of mitochondrial Ca^{2+} influx in the fragmented mitochondria. However, quantification of mitochondrial Ca^{2+} concentration by GEM-GECO1 only reflects the mean value. Using mitochondrial localised CAR-GECO1 in conjunction with visualising the whole mitochondrial network by TagBFP revealed a tendency to higher mitochondrial Ca^{2+} concentration in mitochondria close to the nucleus in the area of the endoplasmic reticulum.

Cytosolic and mitochondrial Ca^{2+} concentrations showed a similar oscillatory pattern in mtNOD mice and decreased overall with ageing, by contrast with controls. It has been shown that SLC25A23 interacts with MCU and induces oxidative stress-mediated cell death [24]. The decrease in SLC25A23 expression with ageing in control mice contrasts with the increase measured in mtNOD mice. This is in line with our previous finding that mitochondrial ROS normalised in control mice after reaching a threshold, but continuously increased in mtNOD mice [25]. Our results indicating a decline in mitochondrial Ca^{2+} concentration with ageing are inconsistent with the suggestion that higher SLC25A23 expression results in higher mitochondrial Ca^{2+} influx [24]. However, the MICU1 to MCU ratio is perhaps more important for mitochondrial Ca^{2+} influx [33] than the absolute expression of SLC25A23 and this ratio declined in mtNOD mice with ageing more than in controls (Figs. 6 and 7). In addition, expression of MICUR1, a positive regulator of MCU, also decreased with ageing. Because mtNOD mice showed age-dependent adaptation with increasing mitochondrial membrane potential and cytochrome c oxidase activity [25], this supports the hypothesis that MICUR1 acts as a direct regulator of mitochondrial Ca^{2+} uptake [16–18,38]. We noted a constant expression of VDAC1, indicating that the pathological threshold of intracellular Ca^{2+} elevation has not been reached. High VDAC1 together with MCU expression has been reported after acute alcohol treatment in rat hepatocytes [34]. A recent review has concluded that during induction of apoptosis intracellular Ca^{2+} increases and augments VDAC1 expression levels [39]. However, our findings in mtNOD mice rather suggest an age- dependent adaptation of Ca^{2+} influx to the mitochondrial network structure. In mtNOD mice we observed an elongated mitochondrial network with some hyper-fusion at 6 and 12 months [25] (Fig. 7). In line with our hypothesis in controls above, the degree of elongation correlated inversely with the Ca^{2+} concentration with ageing. Because of the rapid Ca^{2+} distribution within the network a high level of controllability exists and low Ca^{2+} concentrations are sufficient [37]. Another corroborating argument is the pattern of mitofusin 2 (Mfn2) expression in mtNOD mice with ageing [25]. Mfn 2 tethers mitochondria to the endoplasmic reticulum in dependence of parkin [40]. The Mfn 2 expression pattern in mtNOD mice correlated inversely with the Ca^{2+}

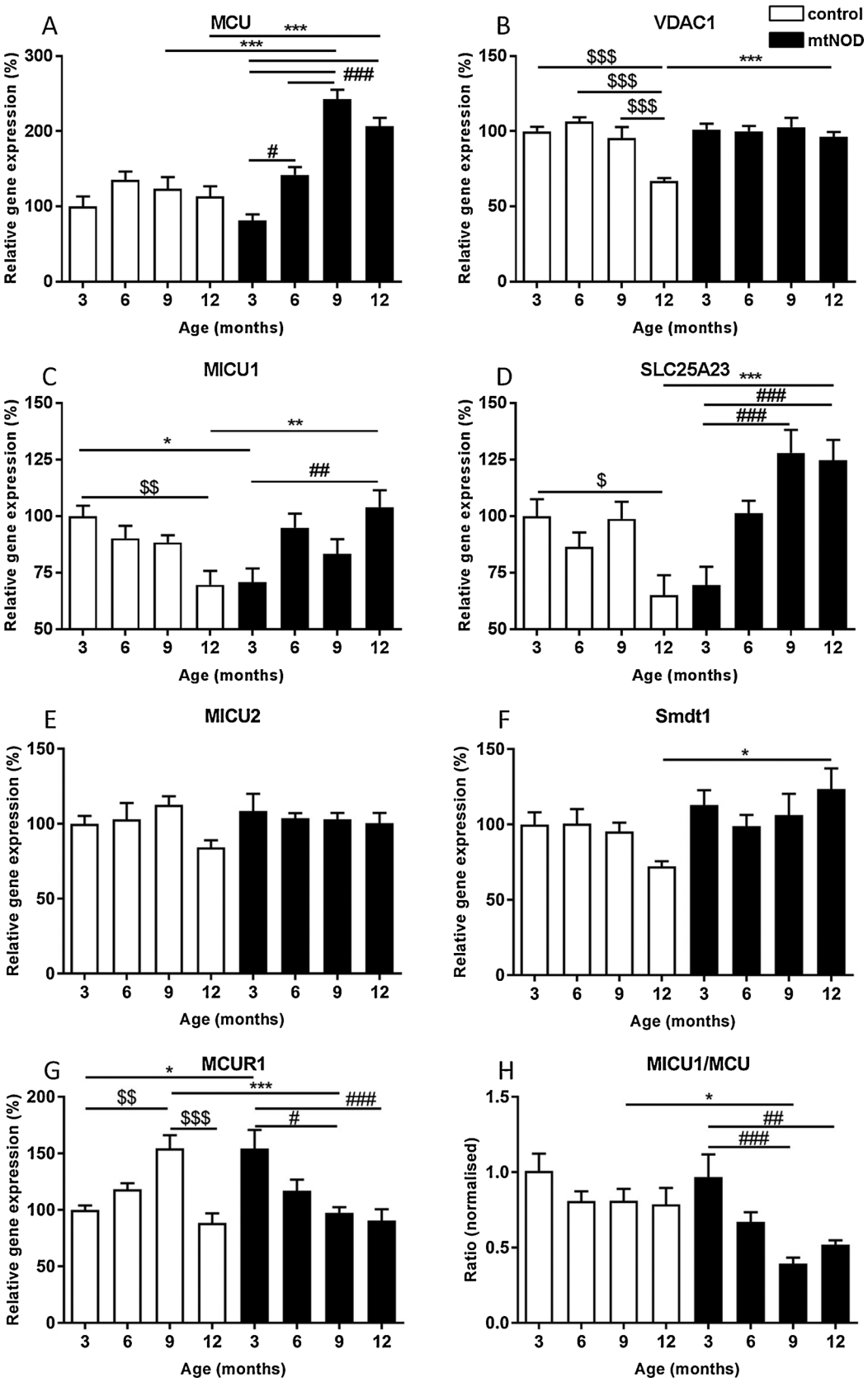

Fig. 6. Gene expression of mitochondrial Ca^{2+} channels and regulatory proteins. Expression of MCU (A), VDAC1 (B), MICU1 (C) and SLC25A23 (D), MICU2 (E), Smdt1 (F), MCUR1 (G) and MICU1/MCU ratio (H) in hepatocytes from 3-, 6-, 9- and 12-month-old control mice (white bars) and mtNOD mice (black bars). Data were calculated in relation to GAPDH expression and normalised to 3-month-old control mice. Values (n = 3) are expressed as mean ± SEM (*, $, # $p < 0.05$; **, $$, ## $p < 0.01$; ***, $$$, ### $p < 0.001$; 1-way ANOVA/Bonferroni's test).

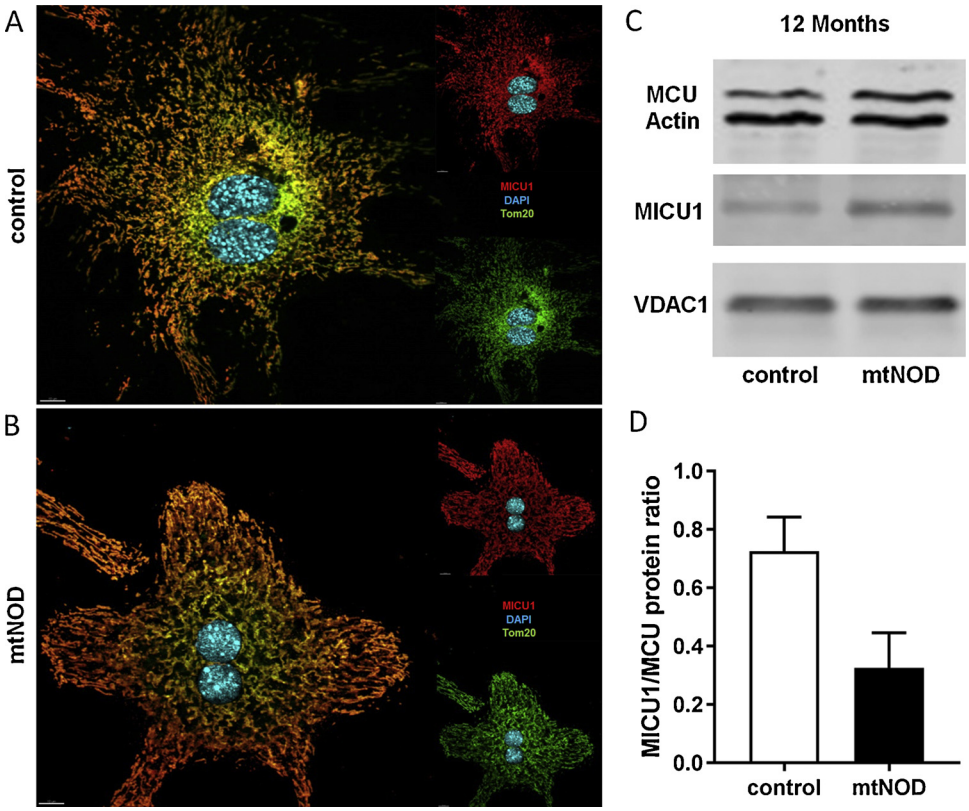

Fig. 7. Protein expression of mitochondrial Ca^{2+} channels and regulatory proteins in 12-month-old mice. Representative images of MICU 1 and Tom20 immunofluorescence in hepatocytes of control mice (A) and mtNOD mice (B) are shown. Tom20 served as a mitochondrial marker. Scale bar: 10 µm. (C) Representative western blots from 3 independent experiments of MCU, actin, MICU1 and VDAC1 expression in control mice (left) and mtNOD mice (right) are shown. (D) The MICU1/MCU protein ratio in control mice (white bar) and mtNOD mice (black bar) was calculated. Values are expressed as mean ± SEM (p = 0.055; Student's *t* test).

concentration pattern [25]. Furthermore we have reported increasing parkin expression with ageing [25].

In conclusion, we have observed evidence in primary mouse hepatocytes to indicate that cytosolic and mitochondrial Ca^{2+} concentrations adjust to age-dependent changes in the mitochondrial network structure and this, in turn, reflects mitochondrial metabolism [25]. Our mtNOD mouse (with more elongated mitochondrial networks than those seen in controls) is an interesting model to further prove the hypothesis that mitochondrial fusion increases the controllability of mitochondrial metabolism by Ca^{2+} [37]. Our study supports the suggestion that the MICU1 to MCU ratio is important for Ca^{2+} influx in hepatocytes [33], but also shows that further studies with special emphasis on MCUR1 are required to elucidate the regulatory principles controlling MCU expression [23].

Author contributions

SB designed the study. JN, CZ and RW researched and analysed data. SB and MT analysed data. JN and SB wrote the manuscript. All authors approved the final version submitted for publication.

Declaration of Competing Interest

The authors declare that there is no conflict of interest.

Acknowledgements

This study was funded by the BMBF GERONTOSYS 2 project ROSAge and the DDG. The authors are indebted to Mr David Beattie (freelance medical writer/UK) for editorial assistance in preparing the manuscript for publication.

References

[1] M. Berridge, M.D. Bootman, P. Lipp, Calcium—a life and death signal, Nature 395 (1998) 645–648.
[2] D. Clapham, Calcium signaling, Cell 131 (2007) 1047–1058.
[3] M. Berridge, The endoplasmic reticulum: a multifunctional signaling organelle, Cell Calcium 32 (2002) 235–249.
[4] A. Thomas, Sharing calcium opens new avenues of signalling, Nat. Cell Biol. 2 (2000) E126–E127.
[5] F. Gellerich, Z. Gizatullina, S. Trumbeckaite, H.P. Nguyen, T. Pallas, O. Arandarcikaite, S. Vielhaber, E. Seppet, F. Striggow, The regulation of OXPHOS by extramitochondrial calcium, Biochim. Biophys. Acta 1797 (2010) 1018–1027.
[6] G. Rutter, R.M. Denton, Regulation of NAD+-linked isocitrate dehydrogenase and 2-oxoglutarate dehydrogenase by Ca2+ ions within toluene-permeabilized rat heart mitochondria. Interactions with regulation by adenine nucleotides and NADH/NAD+ ratios, Biochem. J. 252 (1988) 181–189.
[7] R. Denton, J.G. McCormack, N.J. Edgell, Regulation of mitochondrial dehydrogenases by calcium ions, Biochim. Biophys. Acta 1787 (2009) 1309–1316.
[8] S. Cavero, J. Traba, A. Del Arco, J. Satrústegui, The calcium-dependent ATP-Mg/Pi mitochondrial carrier is a target of glucose-induced calcium signalling in Saccharomyces cerevisiae, Biochem. J. 392 (2005) 537–544.
[9] M. MacDonald, L.J. Brown, Calcium activation of mitochondrial glycerol phosphate dehydrogenase restudied, Arch. Biochem. Biophys. 326 (1996) 79–84.
[10] M. Cleeter, J.M. Cooper, V.M. Darley-Usmar, S. Moncada, A.H. Schapira, Reversible inhibition of cytochrome c oxidase, the terminal enzyme of the mitochondrial respiratory chain, by nitric oxide. Implications for neurodegenerative diseases, FEBS Lett. 345 (1994) 50–54.
[11] M. Ott, J.D. Robertson, V. Gogvadze, B. Zhivotovsky, S. Orrenius, Cytochrome c release from mitochondria proceeds by a two-step process, Proc. Natl. Acad. Sci. U. S. A. 99 (2002) 1259–1263.
[12] A. Halestrap, C. Brenner, The adenine nucleotide translocase: a central component of the mitochondrial permeability transition pore and key player in cell death, Curr. Med. Chem. 10 (2003) 1507-1025.
[13] P. Brookes, Y. Yoon, J.L. Robotham, M.W. Anders, S.S. Sheu, Calcium, ATP, and ROS: a mitochondrial love-hate triangle, Am. J. Physiol. Cell Physiol. 287 (4) (2004) 817–833.
[14] D. Ben-Hail, R. Palty, V. Shoshan-Barmatz, Measurement of mitochondrial Ca2+ transport mediated by Three transport proteins: VDAC1, the Na+/Ca2+ exchanger, and the Ca2+ uniporter, Cold Spring Harb. Protoc. 2014 (2014) 161–166.
[15] M. Litsky, D.R. Pfeiffer, Regulation of the mitochondrial Ca2+ uniporter by external adenine nucleotides: the uniporter behaves like a gated channel which is regulated by nucleotides and divalent cations, Biochemistry 36 (1997) 7071–7080.
[16] K. Mallilankaraman, C. Cardenas, P.J. Doonan, H.C. Chandramoorthy, K.M. Irrinki, T. Golenar, G. Csordas, P. Madireddi, J. Yang, M. Muller, R. Miller, J.E. Kolesar, J. Molgo, B. Kaufman, G. Hajnoczky, J.K. Foskett, M. Madesh, MCUR1 is an essential component of mitochondrial Ca2+ uptake that regulates cellular metabolism, Nat. Cell Biol. 14 (2012) 1336-+.
[17] D. Tomar, Z.W. Dong, S. Shanmughapriya, D.A. Koch, T. Thomas, N.E. Hoffman, S.A. Timbalia, S.J. Goldman, S.L. Breves, D.P. Corbally, N. Nemani,

J.P. Fairweather, A.R. Cutri, X.Q. Zhang, J.L. Song, F. Jana, J.H. Huang, C. Barrero, J.E. Rabinowitz, T.S. Luongo, S.M. Schumacher, M.E. Rockman, A. Dietrich, S. Merali, J. Caplan, P. Stathopulos, R.S. Ahima, J.Y. Cheung, S.R. Houser, W.J. Koch, V. Patel, V.M. Gohil, J.W. Elrod, S. Rajan, M. Madesh, MCUR1 Is a scaffold factor for the MCU complex function and promotes mitochondrial bioenergetics, Cell Rep. 15 (2016) 1673–1685.

[18] H. Vais, J.E. Tanis, M. Muller, R. Payne, K. Mallilankaraman, J.K. Foskett, MCUR1, CCDC90A, Is a regulator of the mitochondrial calcium uniporter, Cell Metab. 22 (2015) 533–535.

[19] K.F. Xie, D.D. Guo, X.J. Luo, SMDT1-driven change in mitochondrial dynamics mediate cell apoptosis in PDAC, Biochem. Biophys. Res. Commun. 511 (2019) 323–329.

[20] H. Vais, K. Mallilankaraman, D.O.D. Mak, H. Hoff, R. Payne, J.E. Tanis, J.K. Foskett, EMRE Is a matrix Ca2+ sensor that governs gatekeeping of the mitochondrial Ca2+ uniporter, Cell Rep. 14 (2016) 403–410.

[21] V. Paupe, J. Prudent, E.P. Dassa, O.Z. Rendon, E.A. Shoubridge, CCDC90A (MCUR1) is a cytochrome c oxidase assembly factor and not a regulator of the mitochondrial calcium uniporter, Cell Metab. 21 (2015) 109–116.

[22] M. Patron, V. Checchetto, A. Raffaello, E. Teardo, D. Vecellio Reane, M. Mantoan, V. Granatiero, I. Szabò, D. De Stefani, R. Rizzuto, MICU1 and MICU2 finely tune the mitochondrial Ca2+ uniporter by exerting opposite effects on MCU activity, Mol Cell. 53 (2014) 726–737.

[23] N. Nemani, S. Shanmughapriya, M. Madesh, Molecular regulation of MCU: implications in physiology and disease, Cell Calcium 74 (2018) 86–93.

[24] N. Hoffman, H.C. Chandramoorthy, S. Shanmughapriya, X.Q. Zhang, S. Vallem, P.J. Doonan, K. Malliankaraman, S. Guo, S. Rajan, J.W. Elrod, W.J. Koch, J.Y. Cheung, M. Madesh, SLC25A23 augments mitochondrial Ca^{2+} uptake, interacts with MCU, and induces oxidative stress-mediated cell death, Mol. Biol. Cell 25 (2014) 936–947.

[25] J. Niemann, C. Johne, S. Schröder, F. Koch, S.M. Ibrahim, J. Schultz, M. Tiedge, S. Baltrusch, An mtDNA mutation accelerates liver aging by interfering with the ROS response and mitochondrial life cycle, Free Radic. Biol. Med. 102 (2017) 174–187.

[26] K.S. Wilson, L.J. Prochaska, Phospholipid vesicles containing bovine heart mitochondrial cytochrome c oxidase and subunit III-deficient enzyme: analysis of respiratory control and proton translocating activities, Arch. Biochem. Biophys. 282 (1990) 413–420.

[27] X. Yu, U. Gimsa, L. Wester-Rosenlöf, E. Kanitz, W. Otten, M. Kunz, S.M. Ibrahim, Dissecting the effects of mtDNA variations on complex traits using mouse conplastic strains, Genome Res. 191 (2009) 159–165.

[28] S. Baltrusch, F. Francini, S. Lenzen, M. Tiedge, Interaction of glucokinase with the liver regulatory protein is conferred by leucine-asparagine motifs of the enzyme, Diabetes 54 (2005) 2829–2837.

[29] J. Wu, L. Liu, T. Matsuda, Y. Zhao, A. Rebane, M. Drobizhev, Y.F. Chang, S. Araki, Y. Arai, K. March, T.E. Hughes, K. Sagou, T. Miyata, T. Nagai, W.H. Li, R.E. Campbell, Improved orange and red Ca^{2} ± indicators and photophysical considerations for optogenetic applications, ACS Chem. Neurosci. 4 (2013) 963–972.

[30] Y. Zhao, S. Araki, J. Wu, T. Teramoto, Y. Chang, M. Nakano, A.S. Abdelfattah, M. Fujiwara, T. Ishihara, T. Nagai, R.E. Campbell1, An expanded palette of genetically encoded Ca2+ indicators, Science 333 (2011) 1888–1891.

[31] O. Subach, I.S. Gundorov, M. Yoshimura, F.V. Subach, J. Zhang, D. Grüenwald, E.A. Souslova, D.M. Chudakov, V.V. Verkhusha, Conversion of red fluorescent protein into a bright blue probe, Chem. Biol. 15 (2008) 1116–1124.

[32] H. Schmitt, S. Lenzen, S. Baltrusch, Glucokinase mediates coupling of glycolysis to mitochondrial metabolism but not to beta cell damage at high glucose exposure levels, Diabetologia 54 (2011) 1744–1755.

[33] M. Paillard, G. Csordas, G. Szanda, T. Golenar, V. Debattisti, A. Bartok, N. Wang, C. Moffat, E.L. Seifert, A. Spat, G. Hajnoczky, Tissue-specific mitochondrial decoding of cytoplasmic Ca(2+) signals Is controlled by the stoichiometry of MICU1/2 and MCU, Cell Rep. 18 (2017) 2291–2300.

[34] G. Wang, E. Memin, I. Murali, L.D. Gaspers, The effect of chronic alcohol consumption on mitochondrial calcium handling in hepatocytes, Biochem. J. 473 (2016) 3903–3921.

[35] S. Groppi, F. Belotti, R.L. Brandão, E. Martegani, R. Tisi, Glucose-induced calcium influx in budding yeast involves a novel calcium transport system and can activate calcineurin, Cell Calcium 49 (2011) 376–386.

[36] T. Albrecht, Y. Zhao, T.H. Nguyen, R.E. Campbell, J.D. Johnson, Fluorescent biosensors illuminate calcium levels within defined beta-cell endosome subpopulations, Cell Calcium 57 (2015) 263–274.

[37] H. Hoitzing, I.G. Johnston, N.S. Jones, What is the function of mitochondrial networks? A theoretical assessment of hypotheses and proposal for future research, BioEssays : news and reviews in molecular, Cell. Dev. Biol. 37 (2015) 687–700.

[38] T.T. Ren, J.J. Wang, H. Zhang, P. Yuan, J.J. Zhu, Y.S. Wu, Q.C. Huang, X. Guo, J. Zhang, L.L. Ji, J.B. Li, H.X. Zhang, H.S. Yang, J.L. Xing, MCUR1-mediated mitochondrial calcium signaling facilitates cell survival of hepatocellular carcinoma via reactive oxygen species-dependent P53 degradation, Antioxid. Redox Signal. 28 (2018) 1120–1136.

[39] V. Shoshan-Barmatz, S. De, A. Meir, The mitochondrial voltage-dependent anion channel 1, Ca(2+) transport, apoptosis, and their regulation, Front. Oncol. 7 (2017) 60.

[40] V. Basso, E. Marchesan, C. Peggion, J. Chakraborty, S. von Stockum, M. Giacomello, D. Ottolini, V. Debattisti, F. Caicci, E. Tasca, V. Pegoraro, C. Angelini, A. Antonini, A. Bertoli, M. Brini, E. Ziviani, Regulation of ER-mitochondria contacts by Parkin via Mfn2, Pharmacol. Res. 138 (2018) 43–56.